ORIGINAL SCIENTIFIC PAPER

CROATICA CHEMICA ACTA

Croat. Chem. Acta **2024**, *97*(4), 175–187
Published online: December 31, 2024
DOI: 10.5562/cca4098

HKD 1926

Synergistic Effect of Additives in $CaCO_3$ Precipitation System at Different Initial pH

Iva Vojtkuf,[1] Marko Andrašić,[2] Damir Kralj,[3] Jasminka Kontrec,[3,*] Branka Njegić Džakula[3,#]

[1] Faculty of Science, University of Zagreb, Horvatovac 102a, 10000, Zagreb, Croatia
[2] J. J. Strossmayer University of Osijek, Department of Chemistry, Ulica Cara Hadrijana 8a, 31000, Osijek, Croatia
[3] Ruđer Bošković Institute, Laboratory for Precipitation Processes, Division of Materials Chemistry, Bijenička cesta 54, 10000, Zagreb, Croatia
* Corresponding author's e-mail address: bnjeg@irb.hr
# Corresponding author's e-mail address: Jasminka.Kontrec@irb.hr
Iva Vojtkuf and Marko Andrašić contributed equally to this work.

RECEIVED: May 9, 2024 * REVISED: June 12, 2024 * ACCEPTED: August 7, 2024

THIS PAPER IS DEDICATED TO THE LATE PROFESSOR TOMISLAV CVITAŠ

Abstract: In this study, the synergistic effect of magnesium ions (Mg^{2+}) and poly-L-aspartic acid (pAsp), at different initial pH (pH_i), on the spontaneous precipitation of calcium carbonate ($CaCO_3$), as a model precipitation system for investigating biomineralization in marine organisms, was investigated. The research was conducted in systems with pH_i from 8.3 to 10.5, molar ratio $n(Mg^{2+}) : n(Ca^{2+}) = 1 : 5$ and pAsp concentration from 1–5 ppm. By comparing synergistic systems with the model system as well as with systems where Mg^{2+} or pAsp were individually added, it was observed that as a consequence of the synergistic effect of Mg^{2+} and pAsp in the entire investigated pH_i range enhanced inhibition of $CaCO_3$ precipitation process occured as well as the change in: polymorphic composition of precipitated $CaCO_3$ and morphology of individual polymorphs. Inhibition of precipitation was intensified with the increase in pH_i, and regarding the polymorphic composition of the precipitate pAsp played a crucial role at lower pH_i while Mg^{2+} was decisive at higher pH_i. These results clearly indicate the significance of pH_i in the synergistic effect of Mg^{2+} and pAsp.

Keywords: calcium carbonate, poly-L-aspartic acid, magnesium, synergy, pH, calcite, vaterite, aragonite, climate change.

INTRODUCTION

CALCIUM carbonate ($CaCO_3$) is one of the most widespread minerals in nature.[1] It forms through precipitation processes, which entail the formation of a new solid phase from a homogeneous system, specifically from aqueous, usually electrolyte solutions, as observed in biological systems.[2] $CaCO_3$ precipitates in the form of six distinct solid phases, yet in marine calcifying organisms (such as mollusks, corals, algae, sponges, foraminifera…) it is typically found in the form of calcium carbonate polymorphs: calcite (the only stable solid phase of $CaCO_3$ at atmospheric pressure and temperatures that dominate the Earth's surface) or aragonite, while vaterite is less common.

This mineral is primary inorganic component in the hard tissues (skeletons, shells…) of these marine organisms, formed during the process of biomineralization.[1] Biomineralization is highly controlled process and precipitation processes are the physical-chemical foundation of biomineralization. Supersaturation stands as the primary precipitation parameter which orchestrates the precipitation of $CaCO_3$. However, various factors wield influence over this process, including the concentrations of constituent ions[3] and the presence of additives[4,5], temperature[6], pH[7,8] or ionic strength[9]. These factors collectively govern the precipitation of $CaCO_3$, thereby impacting biomineralization processes.

As showed in our previous investigation[8], pH is one of the key factors influencing $CaCO_3$ precipitation, inducing changes in its morphology, polymorphic composition and / or precipitation kinetics. In the current context of climate change, understanding the impact of pH on $CaCO_3$ precipitation becomes imperative. Elevated atmospheric CO_2 concentrations lead to increased CO_2 dissolution in

oceans, resulting in ocean acidification and potential $CaCO_3$ dissolution. Since the inorganic part of hard tissues of marine organisms is predominantly composed of calcium carbonate, they are particularly susceptible to acidic environments. The detrimental effect of elevated CO_2 levels on skeletal growth has already been demonstrated.[10,11] Therefore, understanding the effect of environmental parameters, such as pH, on precipitation of $CaCO_3$ and its implications on biomineralizing systems is essential for the verification of carbon cycles and predicting future environmental scenarios.

Numerous inorganic species in marine ecosystems actively participate in biomineralization processes. Non-constituent inorganic ions can enter the crystal lattice, substituting for constituent units and thereby altering the properties of the resulting crystals. Magnesium ion is a very common additive in carbonate and phosphate biominerals. Significance of Mg^{2+} in calcium carbonate biomineralization stems from its chemical similarity to Ca^{2+} and its abundance. It is the most prevalent divalent cation in seawater, with a molar ratio of Mg / Ca of approximately 5.2.[12] It easily incorporates into the calcite lattice (isomorphic substitution of Ca^{2+} for Mg^{2+} in the calcite lattice), inhibiting calcite crystal growth.[13,14] Inhibition becomes significant above the molar ratio of Mg / Ca greater than ~ 1–2.[15] Consequently, the yield of aragonite increases as Mg^{2+} concentration increases.[16] This is typical behavior, observed and described in detail in literature.[13,17,18] Marine calcites, that have incorporated Mg^{2+} in their structure, are categorized as low or high Mg-calcites, based on the boundary of 3–4 mol% Mg incorporated.[19] High Mg calcite, with Mg^{2+} content exceeding 10 mol%, is thermodynamically unstable phase of $CaCO_3$ under ambient conditions.[20] In crystallization experiments, under ambient conditions, when the Mg / Ca molar ratio equals or exceeds 4 (similar to seawater), aragonite, not magnesium calcite, was found to be the kinetically favored $CaCO_3$ crystal phase while at lower Mg / Ca molar ratios, mixtures of calcite, magnesium calcite, and / or aragonite could be obtained.[21,22]

Biominerals, which form hard biomineralized tissues of marine calcifying organisms, besides calcium carbonate, also contain a small amount of organic matter called organic matrix. A critical role of organic matrix in biomineralization process has been recognized long time ago. Organisms secrete organic matrix molecules which become part of the biominerals that build hard tissue of marine calcifying organisms. Organic matrix typically constitutes just few percent of thus formed biomineralized materials, but it is undoubtedly recognized as a key component that regulates the selection of polymorphs or their morphological properties.[1] Such matrices are complex and include insoluble framework macromolecules, usually hydrophobic proteins and polysaccharides[1,23] that control shape, size and aggregation of crystals[24–26] and soluble macromolecules, mostly acidic proteins rich in aspartic and glutamic acid residues[27], that correspond to functional components involved in controlling nucleation, polymorphic selection and growth of the biomineral.[28–30] Many small organic molecules[31–34] and larger species such as polyelectrolytes,[35,36] polyamino acids[37–39] and block copolymers[40,41] were used in controlling calcium carbonate crystallisation and to stabilize amorphous precursor mineral phases. Still, there are many unknowns related to the role of organic matrix and how it affects the crystallization process.

While the focus of presented studies has principally been on the activities of individual additives, crystals in biological systems typically grow under the influence of many different additives. However, only few of biologically inspired studies have addressed the synergistic effects of additives.[42–44] Thus, some authors focused on the synergistic effects of amino acids and coloured dye molecules.[45] They showed that amino acids drive the occlusion of dye molecules at levels that vastly exceed those achieved with the dye alone. These results therefore suggest a novel strategy for generating materials with target properties. Also, investigations of synergistic effect of additives are of particular relevance to biomineralization processes, where multiple additives are invariably present within the biological environment. Polycarboxylates and magnesium ions are thought to play important roles in biomineralization and in the study by Wolf et al.[44], the combination of magnesium ions and polyaspartic acid brings about a pronounced synergistic effect leading to a highly efficient inhibition of particle nucleation and effective stabilization of mineral precursors.

Motivated by these findings, and as continuation of our previous study in which we investigated influence of initial pH on spontaneous precipitation of calcium carbonate[8], we investigated the synergistic effects of poly-L-aspartic acid (pAsp) and Mg^{2+} on the spontaneous precipitation of $CaCO_3$ at different initial pH, under controlled experimental conditions. Our research aims to elucidate how the addition of pAsp and Mg^{2+} influences the nucleation, growth, polymorphism and morphology of precipitated $CaCO_3$ crystals at different initial pH. At that, magnesium ion is used as the non-constituent inorganic ion present in marine ecosystem and known to have an impact on the formation of calcium carbonate biominerals, while pAsp is used as model molecule of naturally occurring soluble acidic macromolecules of organic matrix in biominerals of mollusks. We hypothesis that pAsp and Mg^{2+} will synergistically cause stronger inhibition of nucleation and growth of $CaCO_3$, as well as change the crystal morphology and composition. Also, we assume that this

synergistic effect will depend on the initial pH of the precipitation system.

In today's world, as climate change continues to impact our planet, where ocean acidification is one of the major concerns, understanding the process of calcium carbonate precipitation becomes important, as it represent the physicochemical basis of biomineralization of marine organisms. The results of this research will contribute to the understanding of the fundamental physicochemical mechanisms and regulatory pathways engaged in biomineralization within marine organisms, thereby aiding our response to these environmental challenges.

EXPERIMENTAL

Materials

Analytically pure chemicals $CaCl_2 \times H_2O$, $NaHCO_3$, $MgCl_2$, NaCl, NaOH and poly-L-asparatic acid, M_w (pAsp) = 11100 g mol^{-1} (all chemicals purchased from Sigma–Aldrich, St. Louis, MS, USA) as well as deionized water (conductivity less than 0.055 μS cm^{-1}) were used in experiments.

Spontaneous Precipitation Experiments

Spontaneous precipitation of calcium carbonate in the model system (system without addition of magnesium and/or pAsp) were performed by mixing calcium and carbonate reactant solution: 200 cm^3 of $CaCl_2$ solution was added into 200 cm^3 of solution containing $NaHCO_3$, NaOH and NaCl. NaOH was used to adjust the initial pH (pH_i) of the system and NaCl to fix the ionic strength of the system. In all the systems initial saturation ratio (S) as well as the initial ionic strength (I_c) and solution stoichiometry, were the same. All concentrations of the components in the systems are shown in Table 1.

The experiments were performed in a thermostated (25 °C) double-walled glass vessel tightly closed with a Teflon cover. During the experiments, the systems were continuously stirred at a constant rate by using Teflon–coated magnetic stirring bar. The progress of the precipitation was followed by measuring the pH of the solution using a combined glass-calomel electrode connected to a digital pH meter (PHM 290. Radiometer). After 30 minutes, experiments were finished and the entire solution was filtered through a 0.22 μm cellulose nitrate membrane filter, washed with ultraclear water and dried at 105 °C.

In the systems with the addition of Mg^{2+} (Mg system) an appropriate aliquot of standard $MgCl_2$ solution was added to the calcium solution. The selected ratio of initial amount of magnesium and calcium was $n(Mg^{2+}) : n(Ca^{2+})$ = 1 : 5. All calculated initial concentrations of components in the systems are shown in Table 2.

Table 1. Initial pH (pH_i) and concentration of the components (c) in model systems, with identical ionic strength (I_c = 0.1 mol dm^{-3}), activity ratio ($a(Ca^{2+}) / a(CO_3^{2-})$ = 1.00) and initial saturation ratio (S) with respect to: calcite (S_C = 14.4 ± 0.1), aragonite (S_A = 12.2 ± 0.1) and vaterite (S_V = 7.4 ± 0.1).

pH_i	$NaHCO_3$	$CaCl_2$	NaOH	NaCl
	c / mmol dm^{-3}			
8.30	126.10	4.78	4.49	0.00
9.00	28.30	3.75	4.75	61.70
9.50	12.30	3.66	4.86	77.50
10.00	7.09	3.56	4.89	83.00
10.50	5.50	3.56	5.20	84.20

Table 2. Initial pH (pH_i) and concentration of the components (c), in Mg systems, with identical ionic strength (I_c = 0.1 mol dm^{-3}), activity ratio ($a(Ca^{2+}) / a(CO_3^{2-})$ = 1.00) and initial saturation ratio (S) with respect to: calcite (S_C = 14.9 ± 1.2), aragonite (S_A = 12.6 ± 1.0) and vaterite (S_V = 7.7 ± 0.6).

pH_i	$NaHCO_3$	$CaCl_2$	$MgCl_2$	NaOH	NaCl
	c / mmol dm^{-3}				
8.30	113.00	4.00	0.80	3.79	0.00
9.00	29.90	4.00	0.80	5.23	61.40
9.50	13.40	4.00	0.80	5.47	77.50
10.00	7.99	4.00	0.80	5.62	82.70
10.50	6.28	4.00	0.80	5.97	84.10

In the systems with the addition of pAsp (pAsp system), an appropriate aliquot of the pAsp standard solution was added to the solution containing $NaHCO_3$, NaOH and NaCl. The initial concentrations of pAsp were: 1 ppm, 2 ppm and 5 ppm. All calculated initial concentrations of components in these systems are the same as in the experiments in the model system without the addition of pAsp and are shown in Table 1.

Characterization of Precipitate

The mineralogical composition of the precipitates was analyzed by IR spectroscopy (Tensor II spectrometer, Bruker) using KBr pellets. The mixture of the sample and KBr was previously finely ground and homogenized in a mortar, and then pressed under a pressure of 8 tons for 2 minutes into a pellet with a thickness of 1 mm and a diameter of 1 cm. The IR spectra were measured from 4000 to 400 cm^{-1} with a resolution of 2 cm^{-1} and 32 scans per measurement. The mass fraction of each polymorph in the sample was determined according to the methods for the binary and ternary mixtures of calcium carbonate

polymorphs described in literature.[46,47] From the FT-IR spectra of pure calcite, aragonite and vaterite powders with KBr, the absorptivities, α, of the characteristic absorption band ν_4 for O–C–O bending at 713 cm^{-1} for calcite, 745 cm^{-1} for vaterite, 713 and 700 cm^{-1} for aragonite, were determined. In order to avoid complications arising from the overlap the bands were deconvoluted prior to the determination of respected absorptivities, in the case of the aragonite pellets, or the calculation of the aragonite and calcite crystal phase concentration in the case of ternary mixtures. The results shown represent the average of three measurements. Analysis of a known ternary mixture of calcium carbonate polymorphs tested the validity of the method.

The morphology of the particles was analysed by field emission scanning electron microscopy (JEOL JSM-7000F). Samples were observed as obtained after drying procedure, without coating, fixed on carbon tape. The samples were imaged at acceleration voltage of 5 kV with working distance set at 10 mm, ensuring minimal sample charging.

Data Analysis

Calculations of the solution composition, i.e. the molar concentrations and activities of relevant ionic species, were based on the known total initial concentrations of $CaCl_2$, $NaHCO_3$, NaOH and NaCl and initial pH. The following ionic species were considered: H^+, OH^-, CO_3^{2-}, HCO_3^-, $H_2CO_3^0$, $NaCO_3^-$, $CaCO_3^0$, $CaHCO_3^+$, $CaOH^+$, $CaCl^+$, Ca^{2+}, Na^+, Cl^-, $NaHCO_3^0$, $NaCl^0$, $NaOH^0$. Calculations have been performed by using an algorithm developed within this laboratory and results were compared with those obtained by VMINTEQ 3.0 when possible (available at http://vminteq.lwr.kth.se/download/). The supersaturations were expressed as the saturation ratio, S, defined as the square root of the quotient of the $CaCO_3$ ion activity product, $\Pi = a(Ca2^+) \times a(CO_3^{2-})$, and thermodynamic equilibrium constant of dissolution of the particular $CaCO_3$ phase, $K_{sp}^0 : S = (\Pi / K_{sp}^0)^{1/2}$. The activity coefficients of z–valent ions, y_z, were calculated by using a modification of the Debye–Hückel equation as proposed by Davies[48]. The detailed calculation procedure, which considers the respective protolytic equilibria and equilibrium constants, as well as the charge and mass balance equations, has been described previously.[4,49–51] Equilibrium constants for $CaCl^+$, $NaHCO_3^0$, $NaCl^0$ and $NaOH^0$ were taken from VMINTEQ 3.0.

In all the systems initial saturation ratio (S) as well as the initial ionic strength (I_c) and solution stoichiometry, were the same. The initial saturation ratios (S) of the solutions/systems with the respect to calcite, aragonite, vaterite were: $S_C = 14.4 \pm 0.1$, $S_A = 12.2 \pm 0.1$, $S_V = 7.5 \pm 0.1$ (in model systems and systems with pAsp) and $S_C = 14.9 \pm 1.2$, $S_A = 12.6 \pm 1.0$, $S_V = 7.7 \pm 0.6$ (in systems with Mg^{2+}). The differences between the initial saturation ratio values for these two systems are very small and could be considered the same in all experiments in this work.

Ionic strength (I_c) was set to 0.1 mol dm^{-3} by adjusting the amount of added NaCl. The solution stoichiometry, defined as the ratio of the activities of lattice ions in solution ($a(Ca^{2+}) / a(CO_3^{2-})$), was set to 1.00 by adjusting the amount of $NaHCO_3$ and $CaCl_2$ at the target pH. Initial pH of the systems varied from 8.30 to 10.50 and solution composition of each system is given in the Table 1 and Table 2.

RESULTS AND DISCUSSION

To investigate and draw conclusions regarding the synergistic effect of magnesium ions and pAsp on the spontaneous precipitation of calcium carbonate at different initial pH, the individual influence of each of two additives, magnesium ions and pAsp, has been studied. This involves the analyses of the kinetics of spontaneous calcium carbonate precipitation, changes of the phase composition and morphology of the solid phases resulting from systems containing, either Mg^{2+} or pAsp.

Spontaneous Precipitation of $CaCO_3$ at Different pH_i in the Model System and in the Presence of pAsp or Mg^{2+}

KINETICS AND INDUCTION TIME

Spontaneous precipitation of $CaCO_3$ was monitored by pH measurement, and the initial part of the investigation was conducted on model systems (systems without the addition of Mg^{2+} and / or pAsp). Concentrations of reactants and initial pH of the systems were prepared according to the values shown in Table 1. Experimental curves depicting changes in pH over time during the spontaneous precipitation of calcium carbonate at 25 °C in model systems with different initial pH, but identical initial supersaturation, are shown in Figure 1a. It can be observed that all curves have a similar shape. In the initial part of the pH curve, pH remains relatively constant, and after a certain time (induction time, t_{ind}), precipitation begins, manifested as a significant decrease in pH. In the final part of the pH curve, pH returns to a relatively constant value.

By comparing the presented pH curves, as well as the induction times of model systems with different initial pH, which are shown in Table 3, it is possible to observe that an increase in the initial pH of the system led to an increase in the induction time, indicating a decrease in the rate of $CaCO_3$ nucleation. Namely, the nucleation rate is inversely proportional to the induction time, meaning that the higher the nucleation rate, the shorter the induction time. The

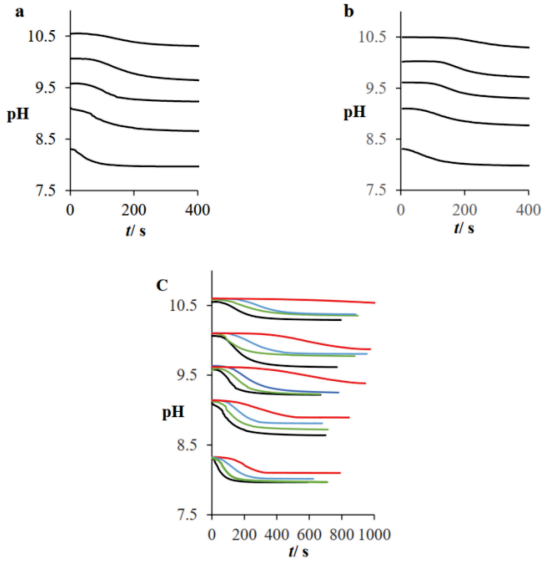

Figure 1. Progress curves, pH versus time, recorded during the spontaneous precipitation of $CaCO_3$ at 25 °C, in: a) model system, b) Mg system, c) pAsp system (– 0 ppm, – 1 ppm, – 2 ppm, – 5 ppm), at identical initial saturation ratio (S_C = 14.4 ± 0.1, S_A = 12.2 ± 0.1, S_V = 7.5 ± 0.1), ionic strength (I_c = 0.1 mol dm^{-3}) and stoichiometry ($a(Ca^{2+})$ / $a(CO_3^{2-})$ = 1.00).

explanation for the observed trend lies in the change in solution composition, i.e., the increase in the concentration of OH^- ions. Based on the previously calculated solution composition and the calculated concentrations of all relevant ionic species present in each individual system at different initial pH, it was observed that the concentration of most ionic species did not change, except for the concentration of hydroxide ions (OH^-), which increased.[8] It is known that hydroxide ions in aqueous solutions are highly hydrated.[52] According to the results of the study by Ruiz-Agudo et al.[7], who investigated the effect of pH on the growth of calcite crystals, the presence of hydroxide ions caused an increase in the frequency of water molecule exchange around Ca^{2+} ions, which consequently, as a dominant effect, caused an increase in interfacial tension, and thus a decrease in the nucleation rate (the nucleation rate is inversely proportional to interfacial tension according to classical nucleation theory[2]), which is precisely what was observed in the studies presented in this work.

The influence of magnesium ions on the spontaneous precipitation of $CaCO_3$ was investigated in the systems with the addition of Mg^{2+}, where $n(Mg^{2+}) : n(Ca^{2+})$ = 1 : 5 (Mg system), at different initial pH. Namely, many literature sources indicate that aragonite formation in geochemical and biological environments is predominantly influenced by the presence of Mg^{2+} ions and at Mg / Ca

Table 3. Induction times (t_{ind}) for the spontaneous precipitation of calcium carbonate in: model system, Mg system and pAsp system, at different initial pH (pH_i).

	t_{ind} / s				
pH_i	Model system	Mg system	pAsp system		
			1 ppm	2 ppm	5 ppm
8.30	30	33	60	120	240
9.00	48	91	80	90	270
9.50	65	156	120	150	630
10.00	72	201	135	220	660
10.50	88	133	150	210	1500

molar ratios higher than 4, while at lower Mg / Ca molar ratios, mixtures of calcite, magnesium calcite, and / or aragonite could be obtained. Therefore, we intentionally applied molar ratio $n(Mg^{2+}) : n(Ca^{2+})$ = 1 : 5 because our preliminary experiments showed that at this molar ratio all three polymorphs precipitated, with special emphasis on vaterite, which was crucial for us in order to be able to study the role of less dominant parameters, like pH and polypeptide addition on possible polymorph selection or morphology.

The concentrations of reactants and initial pH of the systems were prepared according to the values shown in Table 2. Experimental curves depicting changes in pH over time during the spontaneous precipitation of calcium carbonate at 25 °C in systems with different initial pH are shown in Figure 1b. The shape of the curves is the same as in the model systems. Table 3 shows the recorded induction times in these systems. By closely examining the pH curves in Figure 1b and the induction times shown in Table 3, it is possible to observe that, in systems with the addition of magnesium, as well as in model systems, an increase in the initial pH of the system led to an increase in the induction time, indicating a decrease in the nucleation rate of $CaCO_3$. Additionally, comparing the induction times of model systems with the induction times of equivalent systems (same pH_i) with the addition of magnesium (Figure 1b), it can be noticed that the addition of magnesium resulted in an increase in the induction time, indicating a decrease in the nucleation rate compared to the model system. The decreased nucleation rate indicates the inhibitory effect of Mg^{2+} on the precipitation of $CaCO_3$, which is consistent with previous research.[53,54]

The influence of pAsp on the spontaneous precipitation of $CaCO_3$ was investigated in the pAsp systems (systems with the addition of different concentrations of pAsp (1, 2, and 5 ppm), at different initial pH. Figure 1c shows the changes in pH over time for these systems. For comparison, pH curves for the model system are also

shown (black line in Figure 1c). The shape of the curves is similar for all systems, but with increasing pAsp concentration, a smaller decrease in pH and the end of the curve at higher pH was observed. A significant shift in the onset of precipitation was recorded, and induction times and their values are shown in Table 3. For example, at 1 ppm pAsp, the induction time is 60 s at pH_i = 8.3, increasing to approximately 150 s at pH_i = 10.5. Such behavior of the pAsp system is likely a result of crystal growth inhibition, possibly caused by the adsorption of pAsp on the surface of growing crystals.[4,37,55,56]

POLYMORPHISM

To investigate the influence of Mg^{2+} and pAsp on phase composition, FT-IR analysis of the samples spontaneously precipitated in Mg systems or pAsp systems, at different initial pH, was conducted. According to the FT-IR analysis of the samples precipitated in model systems at different pH_i only two solid phases of calcium carbonate, calcite and vaterite, were formed (characteristic absorption bands were observed at 713 cm^{-1} for calcite and 745 cm^{-1} for vaterite). These results are in accordance with our previous investigation.[8] The recorded spectra are shown in Figure 2.

In Figure 3a, the change in the mass fraction of calcite and vaterite with varying initial pH is shown in model systems. It can be observed that at pH 9.0, 9.5, and 10.0, the difference in the mass fraction of calcite in the precipitate is not as pronounced. However, as the pH decreases to 8.3 or increases to 10.5, the mass fraction of calcite in the precipitate significantly increases. Ruiz-Agudo et al.[7] investigated the effect of initial pH (pH ranging from 7.5 to 10.25) on the kinetics of calcite crystal growth on calcite seed crystals and also observed such a nonlinear trend in the kinetics of calcite precipitation, which, as previously described, can be associated with a change in solution composition, i.e., with a change in the concentration of OH^- ions.

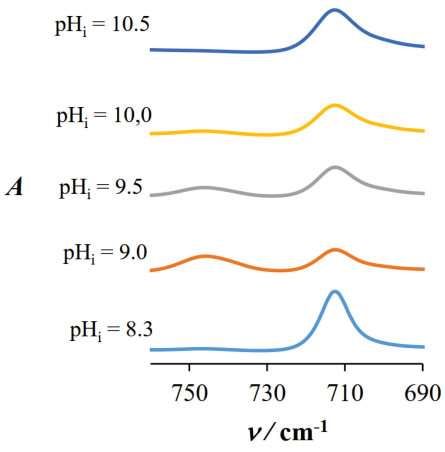

Figure 2. FT-IR spectra of precipitates formed by spontaneous precipitation of $CaCO_3$ in model systems.

To explore the influence of Mg^{2+} on the phase composition of calcium carbonates, FT-IR analysis of samples spontaneously precipitated in Mg systems was conducted: a semi-quantitative analysis of the obtained spectra was performed, and Figure 3b shows the change in the mass fraction of calcite, vaterite, and aragonite with varying initial pH. By comparing the polymorph content (calcite, vaterite, and aragonite) in model systems (Figure 3a) with the content in Mg systems at the same pH_i (Figure 3b), it is possible to observe that the addition of Mg^{2+} to the precipitating systems caused a significant change in the precipitate composition regarding vaterite and aragonite: the fraction of vaterite in the precipitate in Mg systems is lower compared to model systems at the same pH_i, and with an increase in pH_i from 9.0 to 10.5, the fraction of vaterite in the precipitate decreased, indicating that the inhibitory effect of Mg^{2+} on vaterite is stronger at higher pH. Furthermore, the addition of Mg^{2+} to the systems also led to the precipitation of aragonite, unlike in model systems where the formation of aragonite was not observed. With increasing pH_i, the fraction of aragonite in the precipitate also increased. Simultaneously, as the fraction of aragonite in the precipitate increased, the fractions of vaterite and calcite decreased. The explanation for the observed trend lies in the inhibitory effect of Mg^{2+} ions on the crystal growth of vaterite and calcite.[13,14,57] Specifically, Mg^{2+} is incorporated into the crystal structure of calcite and

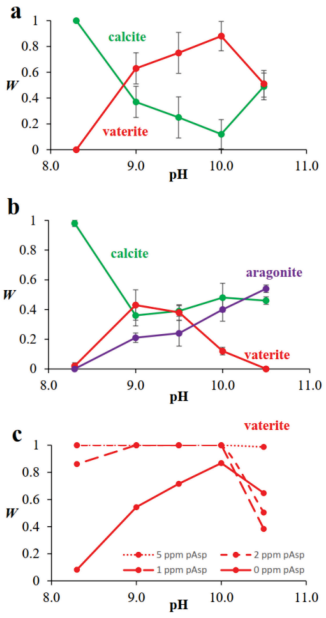

Figure 3. Mass fraction of polymorphs in the precipitate from experiments of calcium carbonate spontaneous precipitation at different initial pH in: a) model system, b) Mg system, and c) pAsp system.

vaterite, causing inhibition of the crystal growth of these two polymorphs.

Therefore, it can be concluded that in systems such as those described in this study, where the prerequisite for the precipitation of all three polymorphs has been achieved (supersaturation with respect to all three polymorphs was relatively high, i.e., $S >> 1$), the addition of Mg^{2+} will cause inhibition of growth of calcite and vaterite, resulting in a decrease in the content of calcite and vaterite in the precipitates and increase in the content of aragonite, as observed in the conducted research.

The addition of pAsp significantly alters the polymorphic composition of the precipitate by increasing the fraction of vaterite in the precipitate (Figure 3c). The change in composition again shows a trend similar to the model system (black line), with higher fractions of calcite at the lowest and the highest pH_i applied (8.3 and 10.5). With the addition of the highest concentration of pAsp (c = 5 ppm), vaterite predominantly precipitates at all investigated initial pH in the system. We showed previously that in the systems in which calcite and vaterite nucleate simultaneously in the absence of additives, the preferential formation of vaterite after the addition of pAsp, pGlu, or pLys, was found to be a consequence of kinetic rather than thermodynamic constraints; strong inhibition of calcite nucleation caused the sole appearance of vaterite.[37]

MORPHOLOGY

To investigate the influence of Mg^{2+} and pAsp on the morphology of spontaneously precipitated $CaCO_3$, scanning electron microscopy was used and the results are shown in Figure 4. If we observe $CaCO_3$ crystals in model system, it is noticeable that at all pH_i, calcite crystals precipitated in the form of rhombohedra with sharp edges (which is a typical shape for calcite crystals), exhibiting overgrown surfaces, and there is no significant difference in the morphology of calcite with changing pH_i. However, the morphology of vaterite changed significantly with increasing pH_i. At pH_i = 9.0, vaterite particles appeared exclusively in the form of cauliflower-like structures; however, with an increase in initial pH, spherical vaterite particles can also be observed. Moreover, with increasing initial pH, the proportion of precipitated vaterite particles in the form of regular spheres increases, while the proportion of vaterite particles in the form of cauliflower structures decreases. At the highest investigated pH_i (10.5), precipitated vaterite predominantly appears as regular spheres. This is also in accordance with our previous investigations about influence of initial pH on $CaCO_3$ precipitation.[8] The morphology of vaterite is diverse and depends on the chemical and physical parameters that determine the precipitation process. As previously discovered, vaterite in the form of regular spheres are aggregates of crystals ranging in size from 25 to 35 nm, while vaterite in the form of cauliflower structures results from subsequent aggregation of these spheres.[58] Although previous studies have examined the effect of pH on vaterite morphology and observed a trend of vaterite precipitation in the form of spheres at higher pH, parameters such as supersaturation, reactant concentration, and the concentration and type of additives were also varied, making it difficult to distinguish the contribution of individual parameters to the morphology of precipitated vaterite. In contrast to those studies, in this work, as well as in our previous research (in which the influence of pH on the precipitation of $CaCO_3$ was investigated) [8] the experimental parameters critical in the precipitation processes, such as supersaturation, ionic strength, temperature, and the ratio of activity of constituent ions, have been identical in all systems. Therefore, the observed effects can be attributed solely to the change in pH_i. Based on the presented results, it can be concluded that an increase in initial pH favors the formation of vaterite in the form of regular spheres. However, unlike in the model systems, no change in the morphology of vaterite was observed in Mg systems and the precipitated vaterite was exclusively in the form of regular spheres, as seen in Figure 4. The presence of only one morphology of vaterite in these systems can be correlated to the incorporation of Mg^{2+} into the vaterite,[57] causing the formation of particles with the same morphology regardless of the initial pH of the system (the effect of Mg^{2+} on vaterite morphology is dominant compared to the effect of pH_i). Additionally, the morphology of aragonite remained unchanged, and in all systems, it was in the form of irregular microaggregates formed by the aggregation of smaller needle-like crystals (Figure 4). For magnesium ions to have influence on aragonite morphology, in systems without any other additives, higher Mg / Ca molar ratio and temperature would have to be applied, as was observed in our previous research.[22]

At the same time, the morphology of calcite, which remained unchanged with varying initial pH in the model systems, changed in Mg systems. Comparing the calcite observed in the model system at pH_i = 8.3 (which was in the form of rhombohedra with sharp edges exhibiting over-grown steps) with calcite precipitated at the same pH in Mg system, it can be observed that the edges became rounded. With further increases in initial pH, irregularly shaped calcite with rounded edges resembling aggregates of smaller rhombohedra of various sizes emerged. The observed change in calcite morphology can be associated with the incorporation of Mg^{2+} into the calcite crystal lattice.[59,60]

The influence of adding 5 ppm pAsp on the morphology of predominantly precipitated vaterite at all

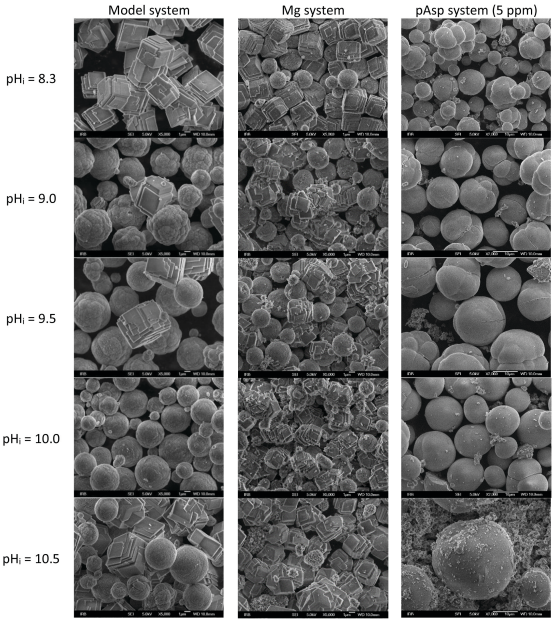

Figure 4. Change of the precipitate morphology with the change of initial pH (pH_i) in the model system, Mg system and pAsp system (c(pAsp) = 5 ppm).

pH_i is shown in Figure 4. Spherical vaterite particles (partially fractured spheres ranging from 3–10 μm) at pH_i = 8.3 resemble cauliflower-like structures with significantly smoothed surfaces. As the pH_i increases, the spheres become more regular, with smoother surfaces and larger sizes (8–15 μm). At the highest pH_i, alongside regular spherical vaterite particles, a significant amount of smaller and irregular vaterite microaggregates were observed. The observed changes in the precipitate composition and vaterite morphology suggest that pAsp affects the nucleation, growth, and aggregation processes of calcium carbonate polymorphs, calcite, and vaterite. It is believed that pAsp binds more strongly to the surface of the stable phase (calcite), causing inhibition of nucleation and growth of calcite, thereby reducing its mass fraction in the systems, and at the highest concentration, completely inhibiting it.[4,37]

Synergistic Effect of pAsp and Mg^{2+} on Spontaneous Precipitation of $CaCO_3$ at Different pH_i

The synergistic effect of dissolved organic molecules and ions is particularly interesting in the field of biomineralization because biomineralization processes always occur in highly complex environments. Contributions to understanding the mechanisms of synergistic effect are also important because they provide better control over crystal growth and properties of crystals precipitated in the presence of multiple additives, as well as for the preparation of new biomimetic materials with special properties and functionalities.[61]

Therefore, we were interested to investigate the effect of pAsp in the presence of magnesium ions in the systems with different initial pH. At that, magnesium ion is used as the non-constituent inorganic ion, known to have significant influence in the formation of calcium carbonate biominerals. Concurrently, poly-L-aspartic acid (pAsp) stands as a representative molecule for the naturally occurring soluble acidic macromolecules found within mollusks biominerals. Figure 5 shows the pH curves for the spontaneous precipitation of calcium carbonate in systems with different initial pH with the addition of c(pAsp) = 5 ppm and

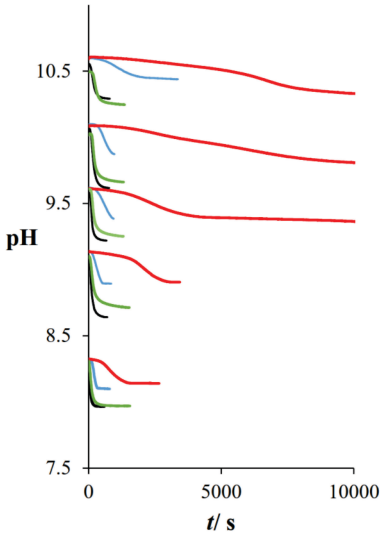

Figure 5. Spontaneous precipitation of calcium carbonate at different initial pH in: model system (black line), Mg system (green line), pAsp system (c(pAsp) = 5 ppm) (blue line) and synergistic Mg–pAsp system (red line).

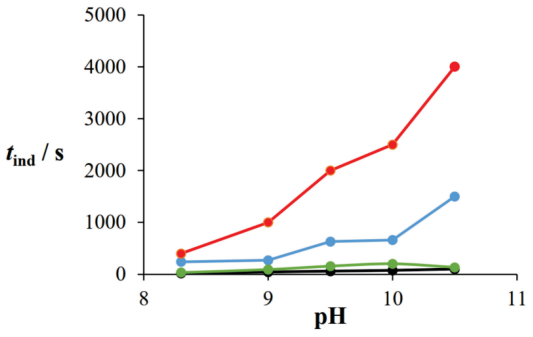

Figure 6. Induction time (t_{ind}) from the experiments of spontaneous precipitation of calcium carbonate at different initial pH in: model system (black line), Mg system (green line), pAsp system (c(pAsp) = 5 ppm) (blue line) and synergistic Mg–pAsp system (red line).

magnesium ($n(Mg^{2+}) : n(Ca^{2+}) = 1 : 5$) – synergistic Mg–pAsp system (red line).

For comparison, in Figure 5 curves which represent the spontaneous precipitation in: model system (black line), Mg system (green line) and pAsp system (c(pAsp) = 5 ppm) (blue line), are also shown. From the shape of the pH curves, it is possible to observe that, when comparing sets of curves recorded at the same pH_i, the induction time is the longest in systems with the addition of both additives, i.e. pAsp and Mg^{2+}. Furthermore, it is noticeable that with an increase in pH_i, the induction time becomes even longer. Figure 6 shows how the induction time increases with increasing initial pH, and again, changes in t_{ind} are shown, for comparison, in: model system (black line), Mg system (green line), pAsp system (c(pAsp) = 5 ppm) (blue line) and synergistic Mg–pAsp system (red line). From the figure 6, it is evident that the highest t_{ind} was measured at the highest initial pH (pH_i = 10.5) in all investigated systems: 88 s (in the model system), 133 s (Mg system), 1500 s (pAsp system (c(pAsp) = 5 ppm)) and 4000 s (synergistic Mg–pAsp system). As mentioned before, an increase in induction time indicates the inhibition of $CaCO_3$ precipitation which in this case means that the inhibition of $CaCO_3$ precipitation was the strongest in the systems where both Mg^{2+} and pAsp were added. Additionally, this inhibition became even more pronounced with the increase in the initial pH of the systems. These results indicate synergistic inhibitory effect of pAsp and Mg^{2+} on the kinetics of calcium carbonate precipitation. According to the literature, observed synergistic effect is most likely caused by stronger hydration of magnesium ions compared to calcium ions, consequently leading to stronger hydration of the amorphous precursor phase, thereby inhibiting the formation of the crystalline phase.[44]

The change in pH in the synergistic Mg–pAsp systems, compared to Mg systems and pAsp system (c(pAsp) = 5 ppm), causes also a significant change in the polymorphic composition of the precipitate (Table 4). In Table 4. phase composition of the precipitates isolated from model system, Mg system, pAsp system (c(pAsp) = 5 ppm) and synergistic Mg–pAsp system, at different initial pH, is shown. In the case of synergistic Mg–pAsp system at pH_i 8.3 and 9.0, vaterite predominates, but with increasing initial pH, the mass fraction of vaterite in the precipitates decreases while the mass fraction of calcite and aragonite increases. At the highest pH 10.5, a mixture of 60 % aragonite and 40 % calcite precipitates. If these results are compared with the results of polymorphic composition of the precipitates isolated from the Mg system and pAsp system (c(pAsp) = 5 ppm), at equivalent pH_i, significant difference could be observed. The greatest difference in the effect on the polymorphism of the precipitate could be observed at lower pH_i, where in the pAsp system (c(pAsp) = 5 ppm) and synergistic Mg–pAsp system, vaterite predominates, while in the model system and in the Mg system, at pH_i = 8.3 calcite predominantly precipitates and at pH_i = 9.0

Table 4. Comparison of the phase composition of the precipitates isolated from: model system, Mg system, pAsp system (c(pAsp) = 5 ppm) and synergistic Mg–pAsp system, at different initial pH.

System	polymorph	pH				
		8.3	9.0	9.5	10.0	10.5
		w (polymorph) / %				
Model	calcite	100	36	26	17	50
	vaterite	0	64	74	83	50
	aragonite	0	0	0	0	0
Mg system	calcite	98	38	40	47	44
	vaterite	2	42	38	13	0
	aragonite	0	20	22	40	50
pAsp system (c(pAsp) = 5 ppm	calcite	0	0	0	0	0
	vaterite	100	100	100	100	98
	aragonite	0	0	0	0	0
Synergistic Mg–pAsp system	calcite	4	3	15	32	40
	vaterite	96	98	73	14	0
	aragonite	0	0	15	54	60

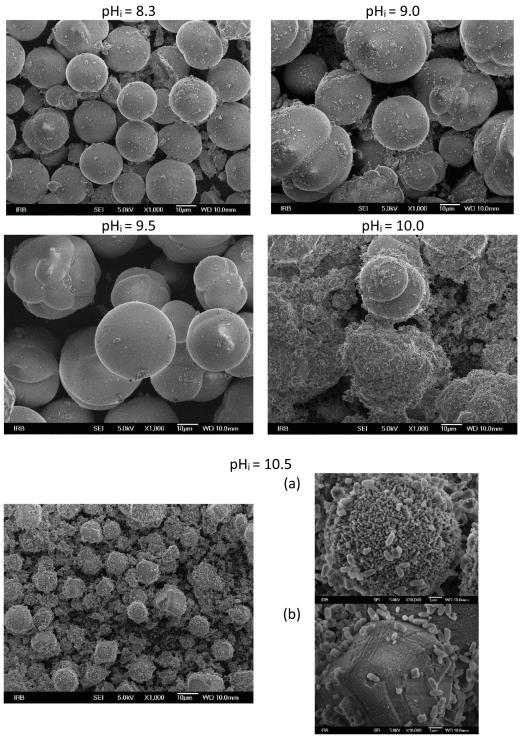

Figure 7. Change of the precipitate morphology with the change of initial pH (pH_i) in synergistic Mg–pAsp system.

mixture of calcite + vaterite precipitates. This indicates that pAsp has a stronger effect on the precipitation process of calcium carbonate at lower pH_i, while at higher pH_i, the effect of Mg^{2+} is stronger, resulting in the predominant formation of a mixture of calcite and aragonite.

The synergistic effect of 5 ppm pAsp and magnesium ($n(Mg^{2+}) : n(Ca^{2+}) = 1 : 5$) on the morphology of precipitated calcium carbonate is shown in Figure 7. Spherical vaterite particles ranging from 10–20 µm predominated at lower pH_i: regular spheres at $pH_i = 8.3$, and a mixture of regular spheres and cauliflower-like spheres at $pH_i = 9.0$ and $pH_i = 9.5$. Also, with the increase of pH_i, size of vaterite particles also increased. At $pH_i = 10.0$ spherical vaterite particles become rare and finally no vaterite is observed at highest investigated pH_i ($pH_i = 10.5$). At $pH_i = 10.0$ and 10.5 calcite and aragonite are dominant phase: aragonite could be observed in the form of spherulitic microaggregates of small needle like crystals (Figure 7, $pH_i = 10.5$, (a)).

Concurrently, morphology of calcite changed significantly. Namely, effect already observed with the addition of only magnesium ions (the rounding of crystal edges of calcite crystals, as a consequence of Mg^{2+} incorporation into calcite crystal lattice, Figure 4) has become much more pronounced, once both, Mg^{2+} and pAsp, have been added into the system, resulting with the irregularly shaped calcite crystals (Figure 7, $pH_i = 10.5$, (b)).

Except for the two mentioned morphologies (irregularly shaped calcite crystals, and aragonite in the form of spherulitic microaggregates of small needle like crystals) a third form has also been recorded as a rod-shaped crystals < 1 µm (Figure 7, $pH_i = 10.5$, (a,b)), which, according to the literature, could be attributed to calcite crystals elongated along the *c*–axis.[60]

CONCLUSIONS

In this study, the synergistic effect of Mg^{2+} and pAsp addition on the spontaneous precipitation of $CaCO_3$ at different initial pH and under conditions of the same initial supersaturation, ionic strength, and activity ratio of constituent ions $a(Ca^{2+}) / a(CO_3^{2-})$, was investigated.

In model systems (systems without Mg^{2+} or pAsp addition), increasing the initial pH in the range from 8.3 to 10.5 resulted in:

- Increased induction time.
- Change in the polymorphic composition of the precipitate: at $pH_i = 8.3$, pure calcite precipitated, then the calcite content decreased, and at $pH_i = 10.0$, vaterite predominantly precipitated, while further increasing pH_i to 10.5, a mixture of calcite and vaterite precipitated in approximately equal proportions.
- Change in the morphology of vaterite particles, but not in the morphology of calcite.

In the precipitation systems with the addition of Mg^{2+} at molar ratio $n(Mg^{2+}) : n(Ca^{2+}) = 1 : 5$ (Mg system), compared to the model system the increase of the pH_i in the range from 8.3 to 10.5 resulted in:

- Increased induction time, which indicates the inhibitory effect of Mg^{2+}.
- Decrease in the mass fraction of vaterite in the precipitates, with this effect further intensified with increasing pH_i. At $pH_i = 10.5$, vaterite does not precipitate.
- Inhibition of calcite precipitation and promotion of aragonite precipitation at $pH_i = 9.0$; with further increase of pH_i mass fraction of aragonite in the precipitates also increased.
- Change in the morphology of calcite particles, but not in the morphology of vaterite and aragonite.

In the systems with the addition of pAsp (pAsp system), compared to the model system, increasing the pH_i in the range from 8.3 to 10.5 resulted in:

- Increased induction time indicating the inhibitory effect of pAsp; the effect is more pronounced with increasing pAsp concentration.

- Increase in the mass fraction of vaterite; at the highest concentration used (5 ppm pAsp) vaterite predominantly precipitates at all tested pH_i.
- Change in the size and morphology of vaterite particles; the size of the spheres increases, their surface becomes smoother, and microaggregates appear alongside them.

In the systems with the addition of both, pAsp and Mg^{2+} (synergistic Mg–pAsp system), compared to the systems with separate addition of Mg^{2+} or pAsp, increasing the pH_i in the range from 8.3 to 10.5 resulted in:

- Additional increase of induction time, which indicates the synergistic inhibitory effect of Mg^{2+} and pAsp.
- Significant change in the polymorphic composition of the precipitate: at pH_i = 8.3 and pH_i = 9.0, vaterite predominantly precipitates.
- At higher pH_i, mass fraction of vaterite in precipitates decreases while mass fraction of calcite and aragonite increases. At pH_i = 10.5, a mixture of 60 % aragonite and 40 % calcite precipitates.
- Significant change in the size and morphology of particles: calcite appeared in a form of irregularly shaped crystals with rounded crystal edges and rod-shaped crystals around 1 μm in size.

The obtained results highlight the synergistic effect of Mg^{2+} and pAsp, which is additionally and significantly influenced by the initial pH of the precipitation system. Thus, pAsp has a stronger effect on the precipitation process of calcium carbonate at lower pH, while Mg^{2+} has a stronger effect at higher pH.

Acknowledgment. This work has been supported by Croatian Science Foundation under the project IP-2013-11-5055.

REFERENCES

[1] S. Mann, *Biomineralization: Principles and Concepts in Bioinorganic Materials Chemistry*, Oxford University Press, New York, **2001**.

[2] Lj. Brečević, D. Kralj, in *Interfacial dynamics (Surfactant science series, vol. 88)*, ed. N. Kallay, Marcel Dekker, New York, **2000**, 435–474.

[3] I. Buljan Meić, J. Kontrec, D. Domazet Jurašin, B. Njegić Džakula, L. Štajner, D. M. Lyons, M. Dutour Sikirić, D. Kralj, *Cryst. Growth Des*. **2017**, *17*, 1103–1117. https://doi.org/10.1021/acs.cgd.6b01501

[4] B. Njegić-Džakula, Lj. Brečević, G. Falini, D. Kralj, *Cryst. Growth Des*. **2009**, *9*, 2425–2434. https://doi.org/10.1021/cg801338b

[5] Lj. Brečević, V. Nöthig-Laslo, D. Kralj, S. Popović, *J. Chem. Soc. - Faraday Trans*. **1996**, *92*, 1017–1022. https://doi.org/10.1039/FT9969201017

[6] P. Jie, L. Zhiming, *PLoS One* **2019**, *14*, 1–17. https://doi.org/10.1371/journal.pone.0223402

[7] E. Ruiz-Agudo, C. V. Putnis, C. Rodriguez-Navarro, A. Putnis, *Geochim. Cosmochim. Acta* **2011**, *75*, 284–296. https://doi.org/10.1016/j.gca.2010.09.034

[8] J. Kontrec, N. Tomašić, N. Matijaković Mlinarić, D. Kralj, B. Njegić Džakula, *Crystals* **2021**, *11*, 1075–1087. https://doi.org/10.3390/cryst11091075

[9] P. Zuddas, A. Mucci, *Geochim. Cosmochim. Acta* **1998**, *62*, 757–766. https://doi.org/10.1016/S0016-7037(98)00026-X

[10] K. J. Kroeker, R. L. Kordas, R. N. Crim, G. G. Singh, *Ecol. Lett*. **2010**, *13*, 1419–1434. https://doi.org/10.1111/j.1461-0248.2010.01518.x

[11] F. Gazeau, C. Quiblier, J. M. Jansen, J.-P. Gattuso, J. J. Middelburg, C. H. R. Heip, *Geophys. Res. Lett.* **2007**, *34*, L07603. https://doi.org/10.1029/2006GL028554

[12] J. M. Astilleros, L. Fernández-Díaz, A. Putnis, *Chem. Geol.* **2010**, *271*, 52–58. https://doi.org/10.1016/j.chemgeo.2009.12.011

[13] K. J. Davis, P. M. Dove, J. J. De Yoreo, *Science* **2000**, *290*, 1134–1137. https://doi.org/10.1126/science.290.5494.1134

[14] R. A. Berner, *Geochim. Cosmochim. Acta* **1975**, *39*, 489–504. https://doi.org/10.1016/0016-7037(75)90102-7

[15] D. Wang, L. M. Hamm, A. J. Giuffre, T. Echigo, J. D. Rimstidt, J. J. De Yoreo, J. Grotzinger, P. M. Dove, *Faraday Discuss*. **2012**, *159*, 371–386. https://doi.org/10.1039/c2fd20077e

[16] W. K. Park, S.-J. Ko, S. W. Lee, K.-H. Cho, J.-W. Ahn, C. Han, *J. Cryst. Growth* **2008**, *310*, 2593–2601. https://doi.org/10.1016/j.jcrysgro.2008.01.023

[17] L. Fernandez-Diaz, A. Putnis, M. Prieto, C. V. Putnis, *J. Sediment. Res.* **1996**, *66*, 482–491.

[18] L. C. Nielsen, J. J. De Yoreo, D. J. DePaolo, *Geochim. Cosmochim. Acta* **2013**, *115*, 100–114. https://doi.org/10.1016/j.gca.2013.04.001

[19] X. Long, Y. Ma, L. Qi, *J. Struct. Biol.* **2014**, *185*, 1–14. https://doi.org/10.1016/j.jsb.2013.11.004

[20] S. Raz, S. Weiner, L. Addadi, *Adv. Mater.* **2000**, *12*, 38–42. https://doi.org/10.1002/(SICI)1521-4095(200001)12:1<38::AID-ADMA38>3.3.CO;2-9

[21] Y. Kitano, D. W. Hood, *J. Oceanogr. Soc. Japan* **1962**, *18*, 141–145. https://doi.org/10.5928/kaiyou1942.18.141

[22] S. Fermani, B. Njegić Džakula, M. Reggi, G. Falini, D. Kralj, *CrystEngComm* **2017**, *19*, 2451–2455. https://doi.org/10.1039/C7CE00197E

[23] S. Mann, *Nature* **1988**, *332*, 119–124. https://doi.org/10.1038/332119a0

[24] L. Addadi, J. Moradian, E. Shay, N. G. Maroudas, S. Weiner, *Proc. Natl. Acad. Sci. U. S. A.* **1987**, *84*, 2732–2736. https://doi.org/10.1073/pnas.84.9.2732
[25] H. Cölfen, *Curr. Opin. Colloid Interface Sci.* **2003**, *8*, 23–31. https://doi.org/10.1016/S1359-0294(03)00012-8
[26] G. Falini, *Int. J. Inorg. Mater.* **2000**, *2*, 455–461. https://doi.org/10.1016/S1466-6049(00)00040-4
[27] B.-A. Gotliv, N. Kessler, J. L. Sumerel, D. E. Morse, N. Tuross, L. Addadi, S. Weiner, *ChemBioChem* **2005**, *6*, 304–314. https://doi.org/10.1002/cbic.200400221
[28] G. Falini, S. Albeck, S. Weiner, L. Addadi, *Science* **1996**, *271*, 67–69. https://doi.org/10.1126/science.271.5245.67
[29] A. M. Belcher, X. H. Wu, R. J. Christensen, P. K. Hansma, G. D. Stucky, D. E. Morse, *Nature* **1996**, *381*, 56–58. https://doi.org/10.1038/381056a0
[30] Q. L. Feng, G. Pu, Y. Pei, F. Z. Cui, H. D. Li, T. N. Kim, *J. Cryst. Growth* **2000**, *216*, 459–465. https://doi.org/10.1016/S0022-0248(00)00396-1
[31] R.-Q. Song, H. Cölfen, *CrystEngComm* **2011**, *13*, 1249–1276. https://doi.org/10.1039/c0ce00419g
[32] W. Jiang, M. S. Pacella, D. Athanasiadou, V. Nelea, H. Vali, R. M. Hazen, J. J. Gray, M. D. McKee, *Nat. Commun.* **2017**, *8*, 15066. https://doi.org/10.1038/ncomms15066
[33] D. C. Green, J. Ihli, Y.-Y. Kim, S. Y. Chong, P. A. Lee, C. J. Empson and F. C. Meldrum, Cryst. Growth Des., 2016, 16, 5174–5183. https://doi.org/10.1021/acs.cgd.6b00741
[34] L. Štajner, J. Kontrec, B. Njegić Džakula, N. Maltar-Strmečki, M. Plodinec, D. M. Lyons, D. Kralj, *J. Cryst. Growth* **2018**, *486*, 71–81. https://doi.org/10.1016/j.jcrysgro.2018.01.023
[35] L. B. Gower, *Chem. Rev.* **2008**, *108*, 4551–4627. https://doi.org/10.1021/cr800443h
[36] Y.-Y. Kim, C. L. Freeman, X. Gong, M. A. Levenstein, Y. Wang, A. Kulak, C. Anduix-Canto, P. A. Lee, S. Li, L. Chen, H. K. Christenson, F. C. Meldrum *Angew. Chemie Int. Ed.* **2017**, *56*, 11885–11890. https://doi.org/10.1002/anie.201706800
[37] B. Njegić-Džakula, G. Falini, Lj. Brečević, Ž. Skoko, D. Kralj, *J. Colloid Interface Sci.* **2010**, *343*, 553–563. https://doi.org/10.1016/j.jcis.2009.12.010
[38] Z. Zou, L. Bertinetti, Y. Politi, P. Fratzl, W. J. E. M. Habraken, *Small* **2017**, *13*, 1603100. https://doi.org/10.1002/smll.201603100
[39] Z. Zou, I. Polishchuk, L. Bertinetti, B. Pokroy, Y. Politi, P. Fratzl, W. J. E. M. Habraken, *J. Mater. Chem. B* **2018**, *6*, 449–457. https://doi.org/10.1039/C7TB03170J
[40] S.-H. Yu, H. Cölfen, *J. Mater. Chem.* **2004**, *14*, 2124–2147. https://doi.org/10.1039/B401420K
[41] Y.-Y. Kim, L. A. Fielding, A. N. Kulak, O. Nahi, W. Mercer, E. R. Jones, S. P. Armes, F. C. Meldrum, *Chem. Mater.* **2018**, *30*, 7091–7099. https://doi.org/10.1021/acs.chemmater.8b02912
[42] M. Li, H. Cölfen, S. Mann, *J. Mater. Chem.* **2004**, *14*, 2269–2276. https://doi.org/10.1039/B400803K
[43] L. A. Bawazer, J. Ihli, T. P. Comyn, K. Critchley, C. J. Empson, F. C. Meldrum, *Adv. Mater.* **2015**, *27*, 223–227. https://doi.org/10.1002/adma.201403185
[44] S. L. P. Wolf, K. Jähme, D. Gebauer, *CrystEngComm* **2015**, *17*, 6857–6862. https://doi.org/10.1039/C5CE00452G
[45] B. Marzec, D. C. Green, M. A. Holden, A. S. Coté, J. Ihli, S. Khalid, A. Kulak, D. Walker, C. Tang, D. M. Duffy, Y. Y. Kim, F. C. Meldrum, *Angew. Chemie - Int. Ed.* **2018**, *57*, 8623–8628. https://doi.org/10.1002/anie.201804365
[46] N. V. Vagenas, A. Gatsouli, C. G. Kontoyannis, *Talanta* **2003**, *59*, 831–836. https://doi.org/10.1016/S0039-9140(02)00638-0
[47] F. A. Andersen, D. Kralj, *Appl. Spectrosc.* **1991**, *45*, 1748–1751. https://doi.org/10.1366/0003702914335292
[48] C. W. Davis, *Ion Association*, Butterworths, London, **1962**.
[49] D. Kralj, Lj. Brečević, A. E. Nielsen, *J. Cryst. Growth* **1990**, *104*, 793–800. https://doi.org/10.1016/0022-0248(90)90104-S
[50] D. Kralj, Lj. Brečević, J. Kontrec, *J. Cryst. Growth* **1997**, *177*, 248–257. https://doi.org/10.1016/S0022-0248(96)01128-1
[51] D. Kralj, Lj. Brečević, A. E. Nielsen, *J. Cryst. Growth* **1994**, *143*, 269–276. https://doi.org/10.1016/0022-0248(94)90067-1
[52] Y. Marcus, *J. Solution Chem.* **1994**, *23*, 831–848. https://doi.org/10.1007/BF00972677
[53] L. Kabalah-Amitai, B. Mayzel, Y. Kauffmann, A. N. Fitch, L. Bloch, P. U. P. A. Gilbert, B. Pokroy, *Science* **2013**, *340*, 454–457. https://doi.org/10.1126/science.1232139
[54] L. Addadi, S. Raz, S. Weiner, *Adv. Mater.* **2003**, *15*, 959–970. https://doi.org/10.1002/adma.200300381
[55] B. Njegić-Džakula, Lj. Brečević, G. Falini, D. Kralj, *Croat. Chem. Acta* **2011**, *84*, 301–314. https://doi.org/10.5562/cca1809
[56] B. Njegić Džakula, G. Falini, D. Kralj, *Croat. Chem. Acta* **2017**, *90*, 689–698. https://doi.org/10.5562/cca3290
[57] P. Bots, L. G. Benning, R. E. M. Rickaby, S. Shaw, *Geology* **2011**, *39*, 331–334. https://doi.org/10.1130/G31619.1

[58] G.-T. Zhou, Q.-Z. Yao, S.-Q. Fu, Y.-B. Guan, *Eur. J. Mineral.* **2010**, *22*, 259–269. https://doi.org/10.1127/0935-1221/2009/0022-2008

[59] K. J. Davis, P. M. Dove, L. E. Wasylenki,J. J. De Yoreo, *Am. Mineral.* **2004**, *89*, 714–720. https://doi.org/10.2138/am-2004-5-605

[60] D. Kralj, J. Kontrec, Lj. Brečević, G. Falini, V. Nöthig-Laslo, *Chem. - A Eur. J.* **2004**, *10*, 1647–1656. https://doi.org/10.1002/chem.200305313

[61] B. Marzec, D. C. Green, M. A. Holden, A. S. Coté, J. Ihli, S. Khalid, A. Kulak, D. Walker, C. Tang, D. M. Duffy, Y. Y. Kim, F. C. Meldrum, *Angew. Chemie - Int. Ed.* **2018**, *57*, 8623–8628. https://doi.org/10.1002/anie.201804365